Origin of Anomalous Lattice Expansion in Oxide Nanoparticles

S. Tsunekawa,[1,*] K. Ishikawa,[2] Z.-Q. Li,[3] Y. Kawazoe,[1] and A. Kasuya[4]

[1]*Institute for Materials Research, Tohoku University, Sendai 980-8577, Japan*
[2]*Research Institute of Electronics, Shizuoka University, Hamamatsu 432-8011, Japan*
[3]*Steacie Institute for Molecular Sciences, National Research Council of Canada,*
100 Sussex Drive, Ottawa, Ontario, Canada K1A OR6
[4]*Center for Interdisciplinary Research, Tohoku University, Sendai 980-8578, Japan*
(Received 16 May 2000)

Anomalous lattice expansions have been measured for the first time in monodisperse CeO_{2-x} nanoparticles and in $BaTiO_3$ single nanoparticles by electron diffraction. X-ray photoelectron spectroscopy studies on CeO_{2-x} nanoparticles and *ab initio* computer simulation on $BaTiO_3$ clusters show that the origin of expansion is the decrease of electrostatic force caused by valence reduction of Ce ions and the increase in ionicity of Ti ions, respectively. The lattice constant change of oxide (ionic) nanoparticles with the increase in ionicity would depend on the structure of the particles. Hence, first-principles calculations of large ionic clusters are indispensable.

Nanocrystalline particles constitute an important class of technologically essential materials. These lie in between clusters, for which a variety of *ab initio* studies have become available, and submicron-sized particles, which have almost the same properties as bulk crystals. Model calculations on large clusters are gradually increasing in number, but *ab initio* (first-principles) computer simulations of clusters composed of more than two elements, and especially large ionic clusters, are very rare. Experimental studies on nanoparticles less than 10 nm in diameter have been regularly carried out in the 1990s. However, data on monodisperse oxide nanoparticles are few and still unreliable.

Recently, we have prepared monodisperse ceria (CeO_{2-x}) [1] and nearly monodisperse barium titanate ($BaTiO_3$) nanoparticles [2]. The half widths at half maximum of the size distributions of these particles are less than 15% and 23%, respectively. Ceria has the fluorite-type structure, mixed valence cations in the bulk crystal, and is a key material for nanosized applications such as ultraviolet absorbing coatings [3], combustion engine promoters [4], and fuel cell electrodes [5]. Barium titanate has the perovskite-type structure, not mixed valence cations, and is the most extensively investigated material among ferroelectrics. Very recently, large lattice expansions have been observed for CeO_{2-x} nanoparticles in toluene suspensions [6,7] and for nanosized single particles of $BaTiO_3$ in ethanol suspensions [8]. This is in contrast to a decrease often observed in the lattice constant of metal nanoparticles with decreasing particle size [9]. We used a transmission electron microscope to obtain the size dependence of the lattice constant from the diffraction rings for CeO_{2-x} particles in the size range of 2–8 nm and from the diffraction spots in various directions for $BaTiO_3$ particles in the size range of 15–250 nm. Here, the particle size is defined as the diameter of the circle equivalent to the area of the image.

The increase in lattice constant with decreasing particle size in nanocrystalline CeO_{2-x} particles [6,7] is connected monotonically with the nominal lattice constant of a maximum size cluster of 14 CeO_2 formula units, composed of Ce^{3+} ions, in spite of the variations strongly depending on the cluster (nominal particle) size [10] (Fig. 1). The nominal lattice constant of clusters composed of Ce^{4+} ions, however, decreases with decreasing cluster size [10], as
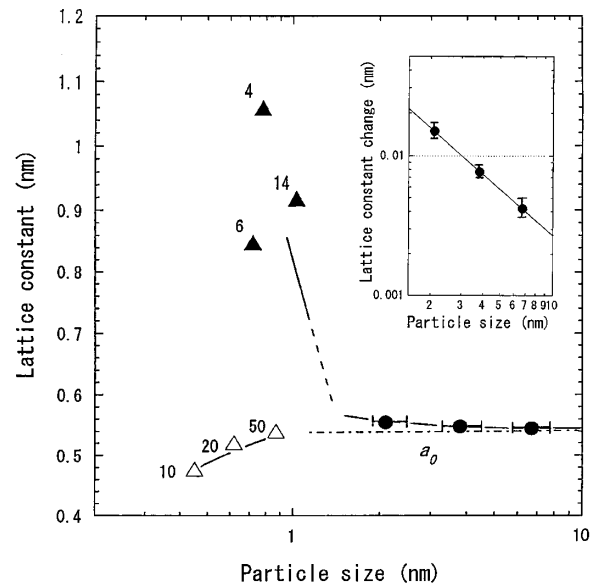

FIG. 1. Size dependences of the fluorite-type lattice constant in CeO_{2-x} nanoparticles (●) (see Ref. [6]), and the nominal lattice constant in the clusters composed of Ce^{4+} (△) and Ce^{3+} (▲) ions obtained from a non-*ab initio* simulation (see Ref. [10]). The nominal lattice constant was estimated as $\sqrt{2}\,d_{Ce\text{-}Ce}$; $d_{Ce\text{-}Ce}$ is the distance of the first nearest neighbor Ce ions, and the nominal particle size was estimated as $(\sqrt{2}\,d_{Ce\text{-}Ce})(n/4)^{1/3}$; n is the number of CeO_2 formula units, as noted next to the open and closed triangles. The inset is a log-log plot of the dependence of lattice constant change on the size of the nanoparticles.

shown in Fig. 1. A log-log plot of the change in lattice constant, Δa, vs the particle size, D, shows a relation of the form $\Delta a = 0.0324 D^{-1.06}$ (nm) for ceria nanoparticles, as shown in the inset. Here, $\Delta a = a - a_0$, and a and a_0 are the lattice constants of the nanoparticles and the bulk crystal [11] (0.5411 nm) at room temperature.

The lattice constant a' in BaTiO$_3$ nanoparticles also monotonically increases with decreasing particle size, while the lattice constant c' decreases slightly with decreasing size and ceases to exist for particle sizes less than 80 nm in diameter [Fig. 2(a)]. A semilogarithmic plot of the change in the lattice constant, $\Delta a'$, against the
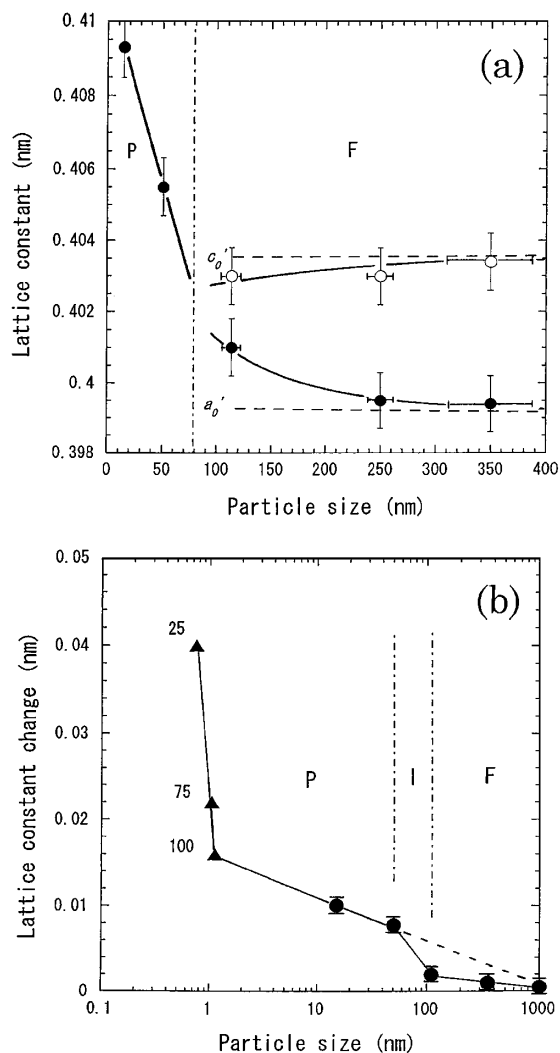

FIG. 2. (a) Size dependence of the lattice constants a' ($\bullet$) and c' ($\circ$) in BaTiO$_3$ nanoparticles (see Ref. [8]). "F" and "P" denote the ferroelectric (tetragonal) and paraelectric (cubic) phases, respectively, and the two dashed lines correspond to the lattice constants of the bulk crystal $a'_0 = 0.399\,20$ and $c'_0 = 0.403\,61$ nm. (b) Semilogarithmic plot of the dependence of lattice constant changes on the sizes of the nanoparticle ($\bullet$) and the cluster ($\blacktriangle$). The lattice constant and particle size in the clusters are obtained from the interatomic distance $d_{\text{Ba-Ti}}$ [see Fig. 3(a)] as alternative $2d_{\text{Ba-Ti}}/\sqrt{3}$ and $(2d_{\text{Ba-Ti}}/\sqrt{3})(N/5)^{1/3}$, respectively, where N is the number of atoms in the cluster as noted next to the triangles.

particle size, D', shows a relation of $\Delta a' = 0.0166 - 0.002\,34 \ln D'$ (nm) for barium titanate nanoparticles. Here $\Delta a' = a' - a'_0$ and a'_0 is the lattice constant [12] (0.399 20 nm) of the bulk crystal. We note that P^{-x} is approximately equal to $1 - x \ln P$, if $x \ln P \ll 1$. It is obtained from Fig. 2(b) as follows: (i) The dilation of a' is suppressed by the ferroelectric phase transition due to a cooperative effect at a critical size of approximately 80 nm, which is the mean value of an intermediate phase "I" between 50 and 110 nm diameter particles and is indicated by an alternate long- and short-dashed line in Fig. 2(a); and (ii) the linear change of the lattice constant of the nanoparticles without the phase transition, as indicated by a dashed line, connects smoothly with that of large clusters, which has been very recently calculated [8] by a cluster model using ab $initio$ ultrasoft pseudopotentials with a plane-wave basis within the local-density approximation. The ferroelectric lattice change at the critical size of nanoparticles has been much discussed as the size-driven phase transition [13,14] or the size-induced diffuse phase transition [15] for the past ten years; the origin of ferroelectricity in the bulk crystals has also been extensively investigated since the 1950s [16,17]. The values of particle sizes and the critical size reported in this Letter are highly reliable due to the direct measurement by electron microscopy rather than the indirect methods of x-ray diffraction and second harmonic generation reported in previous papers [18,19].

The above result (see Fig. 1) strongly suggests that the large lattice expansion in CeO$_{2-x}$ nanoparticles is related to the cluster structure with Ce^{3+} rather than Ce^{4+} ions. The charge reduction from +4 to +3 in Ce ions reasonably results in the lattice expansion due to the electrostatic force reduction. On the other hand, the lattice expansion in BaTiO$_3$ nanoparticles can be connected to the cluster structure with Ti^{4+} ions from the electron density calculation as shown below [Figs. 3(b) and 3(c)].

The Ti-O interatomic distance ($d_{\text{Ti-O}}$) in BaTiO$_3$ is almost constant, being 0.200 nm in the large cluster as well as the bulk [Fig. 3(a)]. It should be noted that, when the character of Ti-O bonds changes from covalent to ionic, $d_{\text{Ti-O}}$ is nearly constant, because the covalent radii of Ti and O for coordination 6 are 0.136 and 0.066 nm, respectively [20]; i.e., the covalent Ti-O distance is 0.202 nm, whereas the corresponding ionic radii are 0.061 and 0.140 nm, respectively [21], leading to nearly the same ionic Ti-O bond length (0.201 nm). A proof of the change of bonding character of Ti ions is obtained from ab $initio$ simulations with pseudopotentials for BaTiO$_3$ bulk crystal and several kinds of clusters. Charge densities in the (001) plane of the bulk crystal are low for Ba ions, but bonding characters are almost completely ionic. Here, Ti ions become almost Ti^{4+}. Therefore, the ionicity in the cluster is nearly the same as that in the bulk for Ba-O bonds, but is strongly increased for Ti-O bonds. These facts demonstrate that the change in the Ti-O bonding character relates to the anomalous expansion of
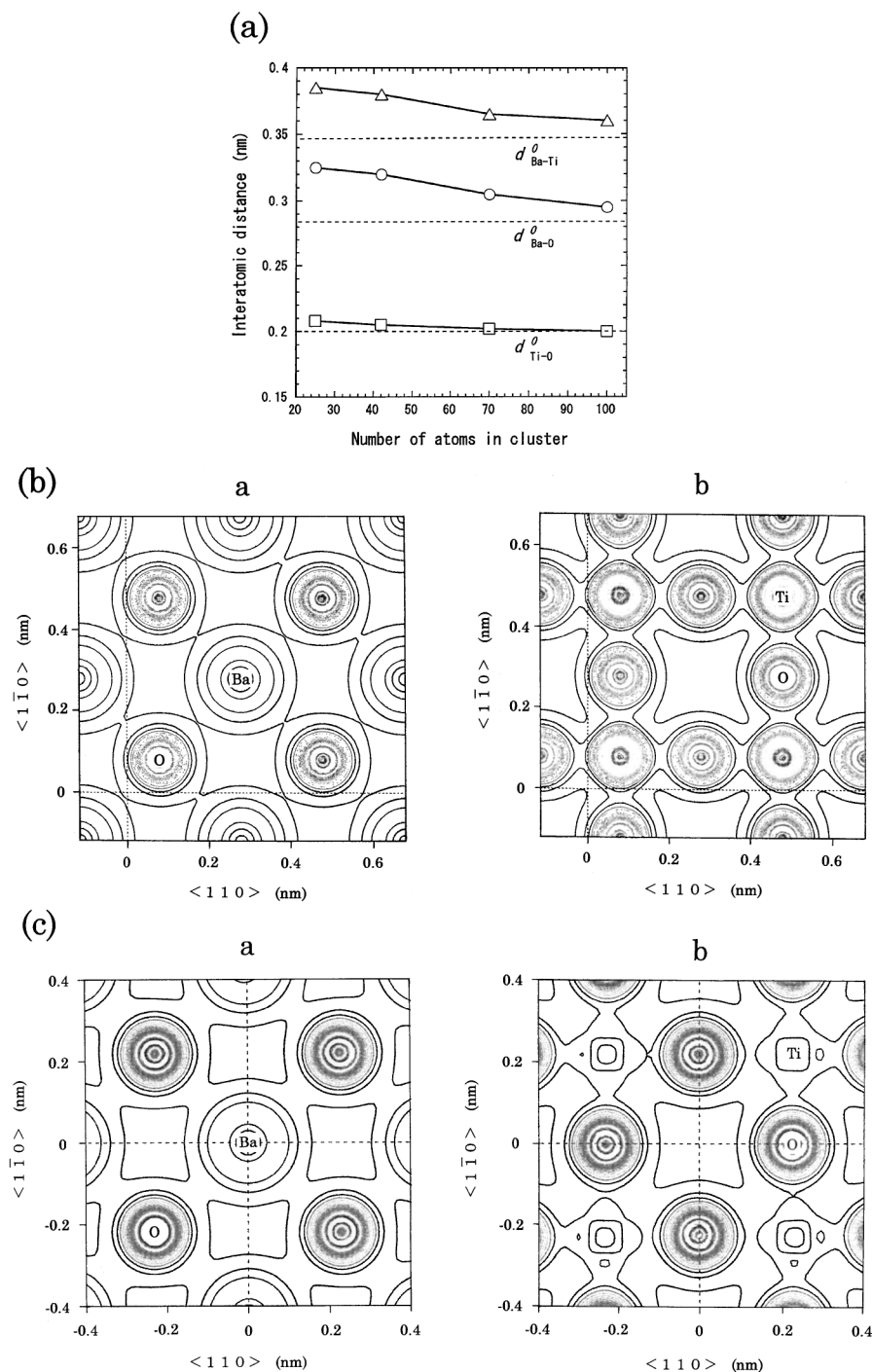
(a)

(b)

(c)

FIG. 3.   *Ab initio* simulation of $BaTiO_3$ clusters.   (a) Dependence of the interatomic distances, d_{Ba-Ti} ($\triangle$), d_{Ba-O} ($\bigcirc$), and d_{Ti-O} ($\square$), on the number of atoms in the clusters, where interatomic distances in the bulk crystal are represented by the dashed lines; i.e., $d^0_{Ba-Ti} = 0.347$, $d^0_{Ba-O} = 0.283$, and $d^0_{Ti-O} = 0.200$ nm. Charge-density plots for Ba, Ti, and O ions in the (001) plane for the bulk crystal (b) and for a cluster of $Ba_{15}Ti_8O_{36}$ (c): a, Ba-O, and b, Ti-O layers.

the nanoparticles, leading to the elongation of Ba-Ti bond lengths owing to the increase in electrostatic repulsion and the consequent expansion of Ba-O bonds.

For ceria nanoparticles, there is a coexistence of Ce^{3+} ions with Ce^{4+} ions as has been recently shown by x-ray photoelectron spectroscopy [22] (XPS) [Fig. 4(a)]. The peaks denoted by SU (shake up) and SD (shake down) are satellites around the Ce^{3+} $3d$ main peaks [23]. The size de-

pendence of the change in lattice constant is in good agreement with that of the valence change of Ce ions, $I(Ce^{3+})/\{I(Ce^{4+}) + I(Ce^{3+})\}$, evaluated by the integrated intensity ratio of the XPS Ce $3d_{5/2}$ peaks as shown in Fig. 4(b). The XPS measurement demonstrates greater reduction of Ce ions with decreasing particle size.

The above results and discussion can be summarized as follows: The lattice constant change in oxide (ionic)
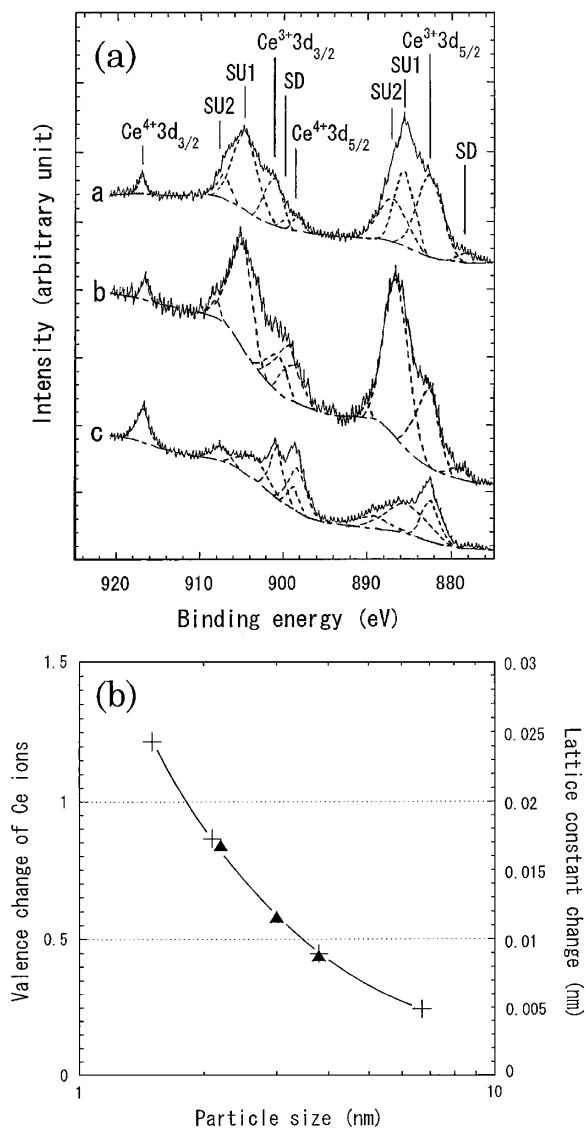
FIG. 4. (a) XPS Ce $3d$ core-level spectra in the following particle sizes: a, 2.2 ± 0.3; b, 3.0 ± 0.4; and c, 3.8 ± 0.6 nm. The peak assignment was after Vercaemst *et al.* (Ref. [23]). (b) Size dependences of the valence change in Ce ions (▲) and the lattice constant change in CeO_{2-x} nanoparticles (+). The former was obtained from the integrated intensity ratio of the main peak of $Ce^{3+} \ 3d_{5/2}$ to $Ce^{4+} \ 3d_{5/2}$.

nanoparticles originates from the variation in nominal ionic valences. The reduction of the valence induces an increase in the lattice constant due to the decrease in electrostatic forces, but the increase in the valence does not always lead to lattice shrinkage. Nanoparticles with the increase in ionicity or nominal valence may show either expansion or shrinkage, depending on the structure of the large clusters, as exemplified here. Therefore, first-principles computer simulations of various kinds of large ionic clusters are indispensable. Lattice constant measurements for the corresponding nanoparticles will then provide a way to determine correlations between the particle size and the surface states through comparison with the simulation results.

———

*Corresponding author.
Email address: scorpion@lexus.imr.tohoku.ac.jp

[1] S. Tsunekawa, R. Sivamohan, T. Ohsuna, A. Kasuya, H. Takahashi, and K. Tohji, Mater. Sci. Forum **315–317**, 439 (1999).

[2] T. Uemori, K. Nagareda, and K. Ishikawa, Bull. RIE Shizuoka Univ. **33**, 91 (1998).

[3] S. Yabe and S. Momose, in *Proceedings of the 3rd Scientific Conference of the Asian Societies of Cosmetic Scientists, Taipei* (Society of Cosmetic Scientists, Republic of China, 1997), p. 103.

[4] A. Trovarelli, Catal. Rev. Sci. Eng. **38**, 439 (1996).

[5] E. P. Murry, T. Tsai, and S. A. Barnett, Nature (London) **400**, 649 (1999).

[6] S. Tsunekawa, R. Sivamohan, S. Ito, A. Kasuya, and T. Fukuda, Nanostruct. Mater. **11**, 141 (1999).

[7] S. Tsunekawa, R. Sahara, Y. Kawazoe, and K. Ishikawa, Appl. Surf. Sci. **152**, 53 (1999).

[8] S. Tsunekawa, S. Ito, T. Mori, K. Ishikawa, Z.-Q. Li, and Y. Kawazoe, Phys. Rev. B **62**, 3065 (2000).

[9] A. Taneda and Y. Kawazoe, J. Magn. Soc. Jpn. **23**, 679 (1999).

[10] H. Cordatos, D. Ford, and R. J. Gorte, J. Phys. Chem. **100**, 18 128 (1996).

[11] JCPDS PDF #34-394.

[12] R. G. Rhodes, Acta Crystallogr. **4**, 105 (1951).

[13] Y. G. Wang, W. L. Zhong, and P. L. Zhang, Solid State Commun. **90**, 329 (1994).

[14] S. Schlag and H.-F. Eicke, Solid State Commun. **91**, 883 (1994).

[15] S. Chattopadhyay, P. Ayyub, R. V. Palkar, and M. Multani, Phys. Rev. B **52**, 13 177 (1995).

[16] Earlier typical work: H. D. Megaw, Acta Crystallogr. **5**, 739 (1952).

[17] Later typical work: R. E. Cohen, Nature (London) **358**, 136 (1992).

[18] M. Tanaka and Y. Makino, Ferroelectric Lett. **24**, 13 (1998).

[19] D. McCauley, R. E. Newnham, and C. A. Randall, J. Am. Ceram. Soc. **81**, 979 (1998).

[20] L. Pauling and M. L. Huggins, Z. Kristallogr. **87**, 205 (1934).

[21] R. D. Shannon and C. T. Prewitt, Acta Crystallogr. Sect. B **25**, 925 (1969).

[22] S. Tsunekawa, T. Fukuda, and A. Kasuya, Surf. Sci. **457**, L437 (2000).

[23] R. Vercaemst, D. Poelman, R. L. Van Meirhaeghe, L. Fiermans, W. H. Laflère, and F. Cardon, J. Lumin. **63**, 19 (1995).